NUMERICAL SIMULATION OF FLOW IN SUPERPAK FAMILY PACKINGS

J. Smutek [1], M. Isoz [1, 2]

[1] **Department of Mathematics, Faculty of Chemical Engineering, University of Chemistry and Technology, Studentska 5, 166 28 Prague, Czech Republic**

[2] **Institute of Thermomechanics of the Czech Academy of Sciences, Dolejskova 5, 182 00 Prague, Czech Republic**

Abstract

The distillation is currently the most energy-intensive technology of the chemical industry. Commonly, the distillation is performed in the columns filled with a structured packing. Structured packings are complex structures used to increase the size of the interface available for the mass transfer. Because of the high complexity of both the packings and the physical phenomena occurring during the distillation, the design of the distillation columns is still based mostly on empirical data. In this work, we concentrate on modeling the gas flow in the SuperPak family of structured packings. First, we propose an algorithm for automatic generation of the packing geometry. Next, we construct and validate a three-dimensional computational fluid dynamics (CFD) model of gas flow through SuperPak 250.Y and SuperPak 350.Y packings. The model validation is done by comparing experimental data of dry pressure losses to the values computed by our model. The obtained difference between the CFD estimates and experiments is bellow 10 %. Finally, we present a parametric study of the SuperPak 250.Y packing geometry. The devised modeling approach may be easily automated and used for optimization of the SuperPak type packing geometry with respect to the gas flow. Furthermore, the proposed CFD model may be extended to account for the multiphase flow.

Keywords: CFD, OpenFOAM, structured packing, distillation, absorption.

1 Introduction

The distillation unit operation is the most energy-consuming process in chemical industry. It is responsible for approximately 50 % of the total energy consumption of industrial separation processes in the US [1]. Therefore, even small improvements in the design of distillation columns will result in considerable cost savings. Commonly, the distillation is performed in the columns filled with a structured packing. Structured packings are geometrically highly complex structures used to increase the size of the interface available for mass transfer. This complexity makes it difficult to investigate physical phenomena occurring during the distillation experimentally. Thus, the design of distillation columns is still based mostly on empirical data.

Computational fluid dynamics (CFD) is a useful tool for the design of structured packings. Already in 1999, the Sulzer company developed a new structured packing, MellapakPlus, using extensive CFD simulations combined with experiments [2]. According to [2] and references therein, the MellapakPlus packing has lower pressure drop and up to 50 % higher maximum useful capacity compared to the conventional Mellapak.

In the present work, we concentrate on modeling the gas flow in a SuperPak family of structured packings. In comparison with other high-performance structured packings, SuperPak packings have three major advantages: lower pressure drop, higher capacities, and better separation efficiency [3]. Unlike other structured packing design, there are no sharp directional flow changes within the SuperPak element. Our approach to model the gas flow in these packings is based on creating a geometry representation that resembles the real packing as much as possible.

Leveraging the periodicity of the structured packings we were able to write an algorithm for automatic generation of the studied packing geometry. We construct and validate a three-dimensional CFD model of gas flow through SuperPak 250.Y and SuperPak 350.Y packings. The model validation is done by comparing experimental data of dry pressure loss to the values computed by our model. Finally, we present a parametric study of the SuperPak 250.Y packing geometry. In this study, a dependence of dry pressure loss on characteristic geometrical parameters of the packing is estimated.

We used the Blender software [4], an open-source 3D creation suite, to generate the packing geometry representation. All simulations were carried out in the OpenFOAM software. OpenFOAM (for "Open source Field Operation And Manipulation") is a C++ toolbox for the solution of continuum mechanics problems, including computational fluid dynamics [5]. The devised modeling approach may be easily automated and used for optimization of the SuperPak type packing geometry with respect to the gas flow. Furthermore, the proposed CFD model may be extended to account for the multiphase flow.

2 SuperPak type packing geometry generation

In this section, we first desribe the geometry of SuperPak family structured packings. Then we present an algorithm for automatic generation of the geometry. SuperPak family packings (see Fig. 1a) consist of N_{sh} metal sheets. These sheets are placed on top of each other to form a cylinder with diameter $D_{pack} = 14$ cm and with height $H_{pack} = 24$ cm. Furthermore, adjacent sheets are flipped by 180° with respect to each other. The sheets are made of rectangular arcs. A series of consecutive arcs forms a channel inclined by an angle θ_{ch} to the horizontal. A channel formed by a series of arcs is depicted in Fig. 2b. Parameters needed to define the SuperPak type packing geometry are (i) width of the arc w_{arc}, (ii) length of the arc l_{arc}, (iii) height of the arc h_{arc}, (iv) distance between two arcs m_{arc}, and (v) thickness of a sheet th_{arc} (see Fig. 2a). The thickness of a sheet could not be measured directly, as the packing surface is irregular. In all simulations we used the value of $th_{arc} = 0.5$ mm. We approximated the shape of the arcs with a part of a cylinder of radius R_{arc} and height th_{arc}. Values of the foretold parameters for SuperPak 250.Y and SuperPak 350.Y packings are listed in Tab. 1.

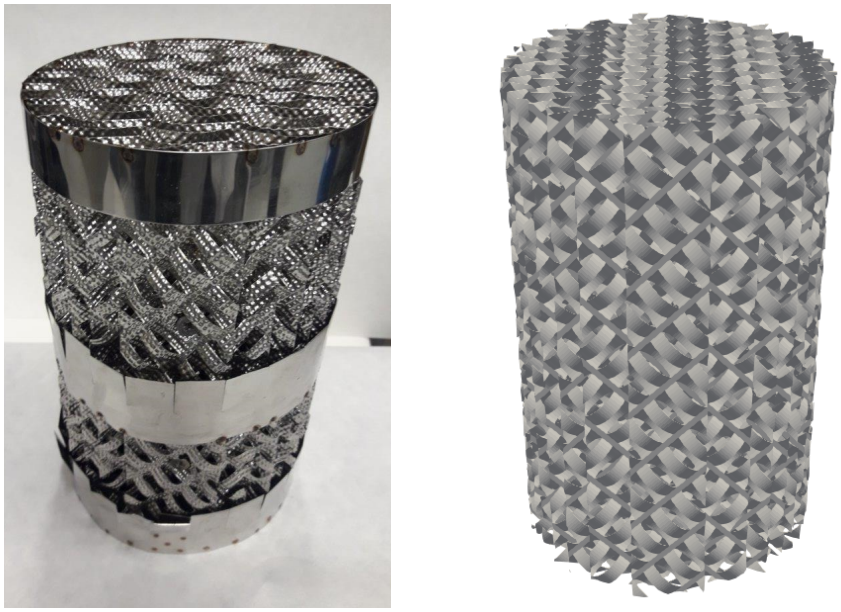

(a) SuperPak packing

(b) Representation of the SuperPak packing

Figure 1: Comparison of laboratory scale SuperPak 250.Y packing and our representation of the packing

The proposed packing generation algorithm can be separated in two parts. In the first part, the algorithm creates a single large sheet template S with $N^y_{arc} = \left\lceil 2\frac{D_{pack}}{w_{arc}} \right\rceil$ arcs in the y axis direction and $N^x_{arc} = \left\lceil 2\frac{H_{pack}}{m_{arc}} \right\rceil$ arcs in the direction of x axis. Then, the first sheet of the packing, S_0 is cut out from the template S. In the second part, the sheet S_0 is duplicated N_{sh} times. Each duplicate is translated on the z axis and cut to fit in the overall cylindrical shape of the packing.

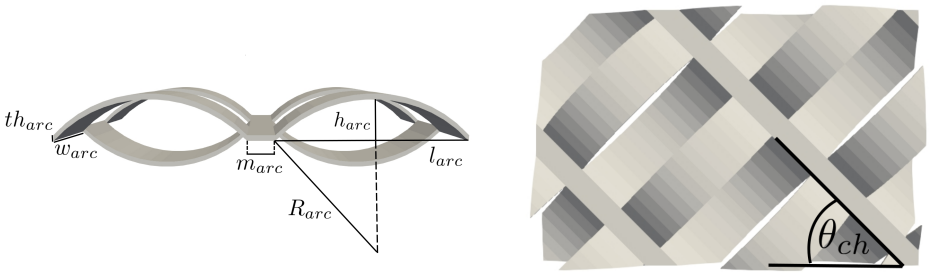

(a) Parameters of SuperPak type packings

(b) Parameter θ_{ch}

Figure 2: Depiction of parameters required to define the SuperPak type packing geometry

Packing	l_{arc}[mm]	w_{arc}[mm]	h_{arc}[mm]	m_{arc}[mm]	N_{sh}
SuperPak 250.Y	18.6	6.9	3.6	2.8	18
SuperPak 350.Y	15.0	5.7	3.0	3.5	22

Table 1: Measured parameters of SuperPak 250.Y and SuperPak 350.Y packings

The packing geometry generation is summarized in Alg. 1. The packing geometry representation is completed by an addition of collars (or wall wipers), consult Fig. 1a.

Algorithm 1 Superpak type geometry generation

Require: Packing geometry parameters: $N^x_{arc}, N^y_{arc}, w_{arc}, l_{arc}, h_{arc}, m_{arc}, \theta_{ch}, N_{sh}, H_{pack}, D_{pack}$

Make a rectangle Re centered at origin with sides $(N^x_{arc}+1)\,w_{arc} \times (N^y_{arc}+1)\,(l_{arc}+m_{arc})$;
for $j = 0$ **to** $N^y_{arc} - 1$ **do**
  Cut a rectangular hole of dimensions $k\,w_{arc} \times l_{arc}$ into Re centered at $S_h = (-(l_{arc}+m_{arc})\,\frac{N^y_{arc}}{2} + j\,(l_{arc}+m_{arc}), 0, 0)$;
  for $i = 0$ **to** $N^x_{arc} - 1$ **do**
    Create an arc $A_{i\,j}$ of dimensions l_{arc} and h_{arc} and with center at $S_{arc} = (-(l_{arc}+m_{arc})\,\frac{N^y_{arc}}{2} + j\,(l_{arc}+m_{arc}), -\frac{w_{arc}}{2}\,N^x_{arc} + i\,w_{arc}, (-1)^i\,(R_{arc}-h_{arc}))$;
  end for
end for
Join all arcs $A_{i\,j}$ and rectangle Re into one sheet $S \leftarrow (\bigcup_{i\,j} A_{i\,j}) \bigcup Re$;
Make a rectangular cuboid Rc with center at origin and of dimensions $D_{pack} \times H_{pack} \times 3h_{arc}$;
Rotate S by an angle θ_{ch} around z axis;
Create first sheet of a packing S_0 by intersecting sheet S with Rc. $S_0 \leftarrow S \cap Rc$;
for $i = 1$ **to** N_{sh} **do**
  Create S_i by copying S_0;
  Translate S_i by $-\frac{(N_{sh}-1)}{2}\,2h_{arc} + 2h_{arc}\,i$ on the z axis;
  if $i \mod 2 = 1$ **then**
    Rotate S_i by π around the y axis;
  end if
  Create a rectangular cuboid Rc_i, centered at origin of dimensions $\sqrt{\frac{D^2_{pack}}{4} - (-(N_{sh}-1)\,h_{arc} + 2h_{arc}\,i)^2} \times H_{pack} \times D_{pack}$;
  Cut S_i by making an intersection of S_i with Rc_i: $S_i \leftarrow S_i \cap Rc_i$;
end for
Create packing P by joining all sheets S_i together: $P \leftarrow (\bigcup_{i=1}^{N_{sh}} S_i)$;
Extrude packing P by th_{arc} in the z axis direction;
return Geometry representation of the packed bed suitable for the snappyHexMesh utility

3 Simulation setup

To estimate dry pressure losses, we need to solve a set of isothermal, turbulent, steady-state Navier-Stokes equations for an incompressible Newtonian fluid [6]. In such a case, the considered equations are (i) the mass conservation equation for an incompressible fluid

$$\nabla \cdot \mathbf{U} = 0\,, \tag{1}$$

where $\mathbf{U}$ stands for the velocity, and (ii) the equation for the conservation of momentum,

$$\nabla \cdot (\mathbf{U} \otimes \mathbf{U}) - \nabla \cdot \mathbb{T} = -\nabla p\,. \tag{2}$$

In equation (2), $\mathbb{T}$ and p denote the viscous stress tensor and the kinematic pressure, respectively. The viscous stress tensor $\mathbb{T}$ is defined as $\mathbb{T} = \nu \nabla \mathbf{U}$, where ν is the fluid kinematic viscosity. Turbulence was taken into account using Reynolds averaged Navier-Stokes equations (RANS) method. Principle of this method lies in expressing the flow variables as a sum of their mean value and fluctuating component as

$$\begin{aligned} \mathbf{U} &= \overline{\mathbf{U}} + \mathbf{U}'\,, \\ p &= \overline{p} + p'\,, \end{aligned} \tag{3}$$

where $\overline{\mathbf{U}}$ and $\overline{p}$ denote the averaged variables and $\mathbf{U}'$ and p' are the instantaneous fluctuations. Substituting from (3) into (1)–(2), we obtain

$$\begin{aligned} \nabla \cdot (\overline{\mathbf{U}} \otimes \overline{\mathbf{U}}) - \nabla \cdot (\overline{\mathbb{T}} + \mathbb{T}') &= -\nabla \overline{p} \\ \nabla \cdot \overline{\mathbf{U}} &= 0\,, \end{aligned} \tag{4}$$

where $\mathbb{T}'$ is the Reynolds stress tensor. The additional stress term $\nabla \cdot \mathbb{T}'$ makes it necessary to solve additional equations in order to close the whole problem. In this work we used the k-ω SST model [7] for the closure of the problem.

The model equations (4) together with the equations for the turbulence variables k and ω were solved via the simpleFoam solver from the OpenFOAM toolbox [5]. This solver uses the SIMPLE (semi-implicit method for pressure linked equations) algorithm of Patankar [8] to manage the coupling of the pressure and velocity equations. In the SIMPLE algorithm, the pressure and velocity fields are updated iteratively in an alternative manner. The applied solution procedure is a segregated one.

The used finite volume (FV) mesh was created via the snappyHexMesh software [9], which is available in the OpenFOAM installation. The snappyHexMesh utility generates 3-dimensional meshes containing hexahedra and split-hexahedra cells automatically from triangulated surface geometries in Stereolithography (STL) format. The needed representation of a packing geometry in STL format was prepared via Alg. 1 implemented in the Blender software [4]. Note that snappyHexMesh can be run in parallel and it also checks the quality of the mesh during the meshing process. These features make the snappyHexMesh utility suitable even for complex geometries such as the SuperPak type packings.

3.1 Boundary conditions

The solved problem definition needs to be completed by suitable boundary conditions. We mark $\mathcal{S}$ the solution domain and $\partial\mathcal{S}$ the boundary of $\mathcal{S}$. The boundary $\partial\mathcal{S}$ can be separated into an inlet $\partial\mathcal{S}_{inlet}$, an outlet $\partial\mathcal{S}_{outlet}$ and walls $\partial\mathcal{S}_{walls}$ as

$$\partial\mathcal{S} = \partial\mathcal{S}_{inlet} \cup \partial\mathcal{S}_{outlet} \cup \partial\mathcal{S}_{walls}\,. \tag{5}$$

The velocity of the gas at the inlet $\mathbf{U} = (0, u_i, 0)^{\mathrm{T}}$ is defined by a Dirichlet type boundary condition. Furthermore, we used a zero-gradient (Neumann) boundary condition for pressure at the inlet.

At the outlet, the so called inletOutlet boundary condition was prescribed for the velocity field $\mathbf{U}$. This condition imposes the zero-gradient (Neumann) boundary condition if $\mathbf{\Phi} = \mathbf{U} \cdot \mathbf{S_f} > 0$,

Boundary	Condition
$\mathcal{S}_{inlet} = \{(x,y,z) \in \mathbb{R}^3 : y = -\frac{H_{col}}{2}, x^2 + z^2 \leq r_{col}^2\}$	$\mathbf{U} = (0, u_i, 0)^{\mathrm{T}}$ $\mathbf{S}_f \cdot \nabla p = 0$ $k = k_0$ $\omega = \omega_0$
$\mathcal{S}_{outlet} = \{(x,y,z) \in \mathbb{R}^3 : y = \frac{H_{col}}{2}, x^2 + z^2 \leq r_{col}^2\}$	$\mathbf{S}_f \cdot \nabla \mathbf{U} = (0,0,0)^{\mathrm{T}}$ if $\mathbf{\Phi} > 0$, $\mathbf{U} = (0,0,0)^{\mathrm{T}}$ else $p = 0$ $\mathbf{\Phi} = \mathbf{S}_f \cdot \mathbf{U}$ $\mathbf{S}_f \cdot \nabla k = 0$ $\mathbf{S}_f \cdot \nabla \omega = 0$
$\mathcal{S}_{walls} =$ packing $\cup$ column hull $\cup$ collars	$\mathbf{U} = (0,0,0)^{\mathrm{T}}$ $\mathbf{S}_f \cdot \nabla p = 0$ $\mathbf{S}_f \cdot \nabla k = 0$ $\mathbf{S}_f \cdot \nabla \omega = 0$

Table 2: Applied boundary conditions. The column height and radius are denoted as H_{col} and r_{col}, respectively. The symbol $\mathbf{S}_f$ marks an outer normal vector to the boundary.

i.e. if the gas flows out of the solution domain. The Dirichlet condition of $\mathbf{U} = (0,0,0)^{\mathrm{T}}$ is used in the opposite case, which prevents the gas from entering at the outlet. The pressure at the outlet was kept constant by a Dirichlet type boundary condition.

The walls part of the boundary comprises the column hull with the packing and the collars. The boundary conditions on the walls are the no-slip boundary condition for the velocity field $\mathbf{U}$ and the zero-gradient condition for pressure p.

Let us note that due to the range of the investigated gas velocities and due the resolution of the used finite volume mesh, the value of $y^+ < 1 \, \forall \boldsymbol{x} \in \partial\mathcal{S}_{walls}$, we did not need to take into account any wall functions for the turbulent variables k and ω. The applied boundary conditions are summarized in Tab. 2. For the exact specification of the boundary conditions for the turbulent variables, especially for the calculation of the values of k_0 and ω_0, we refer the reader to our previous work [10].

4 Results and discussion

4.1 Mesh size independence study

When using finite volume method to numerically solve partial differential equations, it is important to find out the ideal number of cells N_{cells} inside the mesh. If N_{cells} is too small the results will be affected by a significant discretization error. On the other hand, using too many cells in the mesh requires unnecessarily high computational time. To determine the suitable mesh size, we computed dry pressure losses using different numbers of cells in the mesh. We define dry pressure loss as the difference of pressures above and below the packed bed divided by the height of the bed,

$$\Delta p_h = \frac{p_{\text{above}} - p_{\text{below}}}{N_{pack} H_{pack}} \quad \left[\frac{\mathrm{m^2 s^{-2}}}{\mathrm{m}} = \mathrm{m\,s^{-2}}\right]. \tag{6}$$

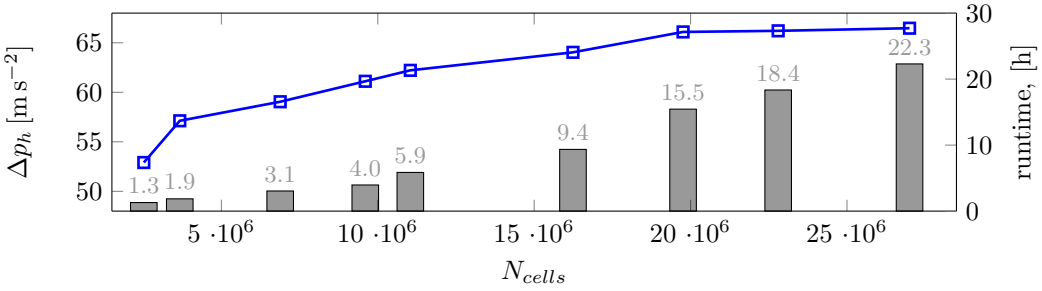

Figure 3: Mesh size independence study of the SuperPak packing

In Fig. 3 we plotted dry pressure drops and simulation runtimes for different values of N_{cells}.

The simulations were carried out on 4 cores of Altix UV2000 commercial cluster [11]. We see, that the pressure drop stabilizes at around 18 milion cells. However, we chose to use around 16 million cells in the mesh since this number offers a good alternative between the discretization error and the computational time.

4.2 Qualitative results

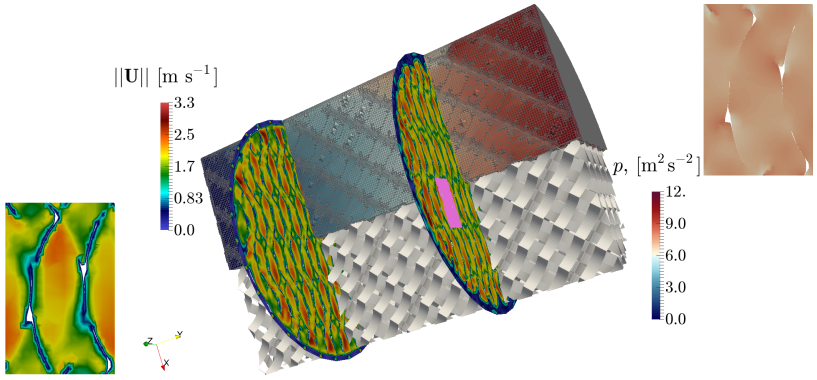

Figure 4: Velocity and pressure fields in the SuperPak 250.Y packing. Details of the velocity and pressure in the highlighted pink area are shown in the bottom left and upper right part of the image, respectively. Inlet velocity was $u_i = 1.5\,\mathrm{m\,s^{-1}}$.

Qualitative results of the simulation of gas flow in one SuperPak 250.Y element are shown in Fig. 4. The velocity field magnitude is shown on the depicted slices, while the pressure field and the structure of the used FV mesh can be seen on the clip in the back. Note the smooth and almost linear change in the pressure along the packing element.

4.3 Model validation

The constructed model was validated by comparing the estimated dry pressure loss to the available experimental data. The experimental data was measured in a semi-industrial column with a diameter $D_{col} = 0.15$ m. The column was filled with 6 packing elements with total height of $H_{col} = 1.41$ m. The used packing elements were SuperPak 250.Y and SuperPak 350.Y. Humidified air was used to measure the dry pressure drop. Density of the air was $\rho_{air} = 1.248$ kg m^{-3} and the air kinematic viscosity was $\nu_{air} = 1.5 \cdot 10^{-6}$ m^{2}s^{-2}. The magnitudes of inlet velocities ranged from $u_i = 0.6\,\mathrm{m\,s^{-1}}$ to $u_i = 3.5\,\mathrm{m\,s^{-1}}$. In our simulations we used only one packing element, since using more than one is computationally expensive and has only a small impact on the results [10].

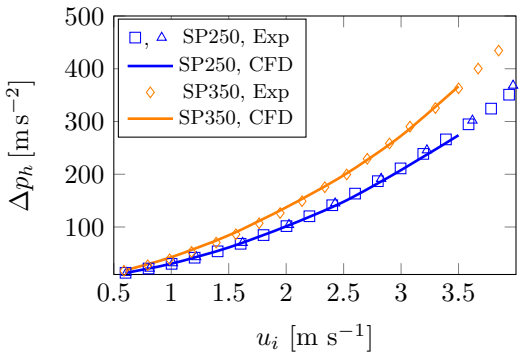

(a) Dependence of pressure drop on inlet velocity

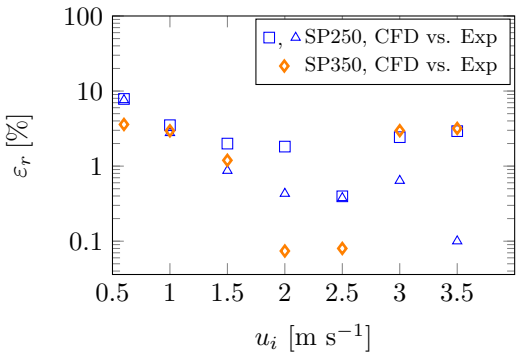

(b) Relative errors of calculated pressure drops

Figure 5: Comparison of measured and computed dry pressure loss.

Results of the validation are shown in Fig. 5. For both packings, the relative error

$$\varepsilon_r = \frac{|\Delta p_h^{CFD} - \Delta p_h^{Exp}|}{\Delta p_h^{Exp}} \cdot 100\% \tag{7}$$

was below 10 %. In Fig. 5b, it can be seen that for SuperPak 250.Y, the error between the CFD and the experiments is comparable to the error between two independent measurements.

4.4 Parametric study

In the last part of the paper, we focus on the dependence of the flow properties on the geometrical parameters of SuperPak 250.Y packing. The studied parameters were the inclination of the channels θ_{ch} and the length of the arc l_{arc}. We created geometries that differed only in the values of studied parameters. Next, we compared the dry pressure losses computed using each geometry. Since we are interested in the qualitative effects of the studied geometry alterations on the flow, we base our comparison on the normalized dry pressure loss,

$$(\Delta p_h)_n^i = \frac{\Delta p_h^i - \min_{(i)} \Delta p_h}{\max_{(i)} \Delta p_h - \min_{(i)} \Delta p_h}\,, \tag{8}$$

where we denoted the current value by the superscript i and all the available values of interest as (i). The values of minimal and maximal dry pressure losses, which are necessary for the calculation of the normalized dry pressure drops, are written in Tab. 3. The results of the parametric study

Varied parameter	u_i [m s^{-1}]	$\max_{(i)} \Delta p_h$ [m s^{-2}]	$\min_{(i)} \Delta p_h$ [m s^{-2}]
θ_{ch}	1.50	66.26	44.55
θ_{ch}	2.25	153.88	100.14
θ_{ch}	3.00	229.78	144.55
l_{arc}	1.50	72.88	56.48
l_{arc}	2.25	147.52	114.52
l_{arc}	3.00	245.00	190.49

Table 3: Maximal and minimal values of dry pressure drops for studied cases.

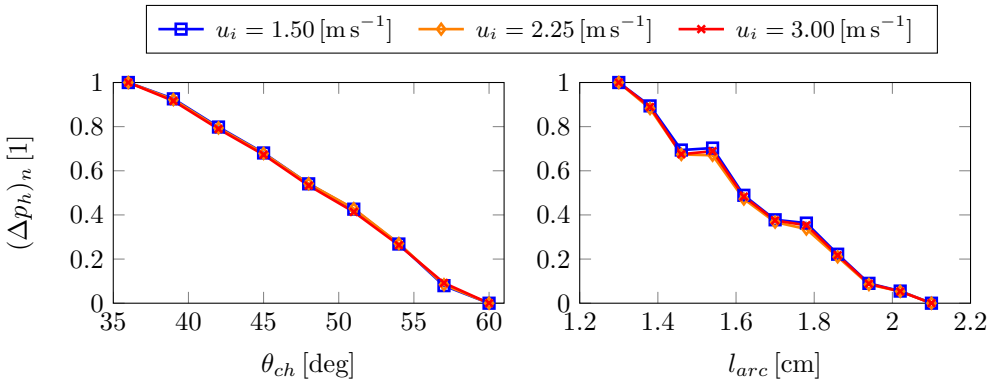

(a) $\Delta(p_h)_n$ as function of θ_{ch} (b) $\Delta(p_h)_n$ as function of l_{arc}

Figure 6: Parametric study of SuperPak 250.Y packing.

are shown in Fig. 6a. The dry pressure loss decreased with the increase in θ_{ch}. Also, there was no considerable change in the trend, when different gas inlet velocities were used. However, there seems to be a slight change in the slope of the dependence of $(\Delta p_h)_n$ on θ_{ch} for $\theta_{ch} \approx 57°$. We attribute this to an appearance of channels that pass the column without encountering the hull.

The dependence of dry pressure loss on the l_{arc} is more complicated (see Fig. 6b). The size of one channel decreases when l_{arc} is decreased, therefore we may expect higher pressure losses for smaller values of l_{arc}. However, there is a visible step in the trend for $l_{arc} \approx 1.5$ cm and $l_{arc} \approx 1.75$ cm . We believe that, this is caused by a formation of new channels around these values of l_{arc}.

5 Conclusions

Distillation is still the most energy-intensive technology of the chemical industry. Structured packings are commonly used in distillation columns, yet their design is based mostly on empirical data. In this work, we provided a quick way to model gas flow inside structured packings. An algorithm for automatic generation of the SuperPak type packing geometry was presented and a three-dimensional CFD model was constructed. The model was validated by comparing experimental data of dry pressure losses to the values computed by the model. At last, we conducted a parametric study of SuperPak 250.Y geometry. In this study we estimated the dependence of the dry pressure loss on the inclination of channels and on the size of one channel. In the future work, we plan to extend our model to account for multiphase flow in the SuperPak packings.

Acknowledgment

This work was supported by The Ministry of Education, Youth and Sports from the Large Infrastructures for Research, Experimental Development and Innovations project "IT4Innovations National Supercomputing Center– LM2015070". The work of M. Isoz was supported by the Centre of Excellence for nonlinear dynamic behaviour of advanced materials in engineering CZ.02.1.01/0.0/0.0/15_003/0000493 (Excellent Research Teams) in the framework of Operational Programme Research, Development and Education. Finally, the authors would like to express theirs deepest thanks to the Mass Transfer Laboratory of UCT Prague for providing experimental data for the model validation as well as for granting an access to their experimental equipments and for many helpful consults on the studied topic.

References

[1] Materials for Separation Technologies: Energy and Emission Reduction Opportunities. Technical report, U.S. Departmesnt of Energy's Office of Energy Efficiency and Renewable Energy, 2005. `https://www1.eere.energy.gov/manufacturing/industries_technologies/imf/pdfs/separationsreport.pdf`.

[2] L. Spiegel and W. Meier. Distillation columns with structured packings in the next decade. *Trans IChemE*, 81(1):39–47, 2003.

[3] M. Schultes. Raschig Super-Pak Eine neue Packungsstruktur mit innovativen Vorteilen im Vergleich. *Chemie Ingenieur Technik*, 80(7):927–933, 2008.

[4] Blender Foundation. Blender. `https://www.blender.org`, visited 2017-12-19.

[5] OpenCFD Ltd. Openfoam. `https://www.openfoam.com`, visited 2017-12-19.

[6] F. Moukalled, M. Darwish, and L. Mangani. *The finite volume method in computational fluid dynamics: an advanced introduction with OpenFOAM and Matlab*. Springer-Verlag, Berlin, Germany, 1st edition, 2016. ISBN 978-3-319-16874-6.

[7] F. R. Menter. Two-equation eddy-viscosity turbulence models for engineering applications. *AIAA*, 32(8):1598–1605, 1994.

[8] S. V. Patankar. *Numerical heat transfer and fluid flow*. Hemisphere publishing, United States, 1 edition, 1980. ISBN 0-07-048740-5.

[9] OpenCFD Ltd. Mesh generation with the SnappyHexMesh utility. `https://www.openfoam.com/documentation/user-guide/snappyHexMesh.php`, visited 2017-12-01.

[10] M. Isoz. CFD study of gas flow through structured separation solumns packings Mellapak 250.X and Mellapak 250.Y. In D. Simurda and T. Bodnar, editors, *Proceedings of the conference TPFM'17, Topical Problems of Fluid Mechanics*, pages 171–184. IT CAS, 2017.

[11] SGI Gobal Sales and Support. SGI UV 2000: Data sheet. Technical Report 4552 12102015, SGI, 2015.